Magnetic ground state of plutonium dioxide: DFT+U calculations

Yue-Fei Hou(侯跃飞)[1], Wei Jiang(江伟)[1], Shu-Jing Li(李淑静)[2], Zhen-Guo Fu(付振国)[1], and Ping Zhang(张平)[1,3,†]

[1] *Institute of Applied Physics and Computational Mathematics, Beijing* 100088, *China*
[2] *Beijing University of Chemical Technology, Beijing* 100029, *China*
[3] *School of Physics and Physical Engineering, Qufu Normal University, Qufu* 273165, *China*

(Received 23 August 2022; revised manuscript received 28 October 2022; accepted manuscript online 31 October 2022)

The magnetic states of the strongly correlated system plutonium dioxide (PuO_2) are studied based on the density functional theory (DFT) plus Hubbard U (DFT+U) method with spin–orbit coupling (SOC) included. A series of typical magnetic structures including the multiple-k types are simulated and compared in the aspect of atomic structure and total energy. We test LDA, PBE, and SCAN exchange–correlation functionals on PuO_2 and a longitudinal 3k antiferromagnetic (AFM) ground state is theoretically determined. This magnetic structure has been identified to be the most stable one by the former computational work using the hybrid functional. Our DFT+U+SOC calculations for the longitudinal 3k AFM ground state suggest a direct gap which is in good agreement with the experimental value. In addition, a genetic algorithm is employed and proved to be effective in predicting magnetic ground state of PuO_2. Finally, a comparison between the results of two extensively used DFT+U approaches to this system is made.

Keywords: strongly correlated system, magnetic ground state, noncollinear, MagGene

PACS: 71.27.+a, 71.15.Mb, 75.10.Dg **DOI:** 10.1088/1674-1056/ac9e96

1. Introduction

Some of the actinide oxides (XO_2, X = U, Np, Pu, Am, *etc*.), as typical strongly correlated systems, normally form the cubic fluorite structure with an $Fm\bar{3}m$ (225) space group.[1] These series of compounds are either Mott insulators or charge-transfer insulators and they provide outstanding platforms to study the properties of localized 5f electrons. Now that the 5f orbits are partially filled in these systems, nonzero magnetic moments can be naturally imagined. Meanwhile, with the presence of spin–orbit coupling (SOC) and cubic crystal field effect, the magnetism of these actinide oxides is expected to be even abundant and complex.

Years before, the magnetic ground states of these actinide oxides had been a fundamental topic causing much discussion.[2] Today experimental evidences of the triple-k (3k)-type magnetic ground states for UO_2 and NpO_2 have been reported in literatures.[3–9] However, different from the Curie–Weiss susceptibility found in UO_2[10] and NpO_2,[11] a temperature-independent susceptibility[12] is observed in PuO_2. What is more, the nuclear magnetic resonance (NMR) experiments[13–15] imply no magnetic order occurred in PuO_2 at low temperature. Surprisingly, a simple crystal field (CF) theory successfully explains the non-magnetic picture of PuO_2.[2] In response, inelastic neutron scattering spectrum (INSS) confirms the transition from the Γ_1 singlet state to the Γ_4 triplet state (*i.e*., the CF ground state to the first excited state) of PuO_2 with a peak at 123 meV.[16] Based on a local density approximation (LDA) calculation to density functional theory (DFT),[17] the Γ_1 state is 99 meV lower than the Γ_4 state. Another LDA calculation combined with exact diagonalization (LDA+ED) of the Anderson impurity model[18] suggests a gap of 126 meV between the two states. These theoretical results are considered to be in reasonable agreement with the INSS. Until here, the nonmagnetic ground state of PuO_2 seems to be clear. However, one abnormal issue is that the experimental susceptibility is much smaller (about 50%) than that of one would expect from the van Vleck coupling of the Γ_1 with the Γ_4.[2,12,16,18] Although the multiconfigurational wave function calculations[19] reproduces the experimental susceptibility of PuO_2, more discussions are required to ensure this achievement. Anyway, the magnetism of PuO_2 needs more investigations from both experimental measurements and theoretical modeling.

In fact, PuO_2 is a challenging system to investigate in experiments duo to its nucleonic radioactive decay and the inhomogeneity of the samples.[20–23] As a result, a series of computational works have been carried out to understand the ground state properties of this system in-depth. Before further simulation of its properties, a reasonable magnetic model for the ground state of PuO_2 is firstly required. For instance, by assuming a simple nonmagnetic (NM), ferromagnetic (FM) or collinear antiferromagnetic (AFM) ground state, many fundamental physical characters of PuO_2, including electronic,[24–28] optical,[27,29] thermodynamic,[27,30] lattice dynamic,[24,31] and surface[24,32–34] properties, have been studied through first-principles calculations. Among them,

†Corresponding author. E-mail: zhang_ping@iapcm.ac.cn

© 2023 Chinese Physical Society and IOP Publishing Ltd

DFT-based calculations are especially popular to study PuO_2 due to its balance between accuracy and economy.

It has been revealed that conventional DFT or even DFT+U calculations tend to provide rather an FM or a collinear AFM ground state[24–28] than the recognized nonmagnetic state by comparing their free energies. To theoretically obtain a nonmagnetic ground state, the modified LDA calculation[18] seems to succeed while CF parameters obtained from the experiment are applied which makes the computational work not totally *ab initio*. On the other hand, it may also be meaningful to leave out the energy difference between magnetic or nonmagnetic states and directly impose a nonmagnetic state in the calculation. For instance, by taking into account SOC and Hubbard U modifications, DFT+U calculations for the nonmagnetic PuO_2 are performed[35,36] and useful results are gained. Despite all this, the consistency between the real ground state and the simulated ground state is of great significance to the applicability of DFT. Only with this robust consistency could we then safely predict other similar systems by using the DFT based methodology. Hence, the ground state of PuO_2 belonging to the DFT framework is required to be determined and examined carefully. Pegg *et al.*[20] calculated the total energy of PuO_2 with different magnetic structures and found a noncollinear longitudinal 3k AFM ground state by using HSE06 hybrid density functional. Nonmagnetic state matches much higher energy than magnetic states in their calculations. The origin of the inconsistency occurred in a series of DFT-based studies[24–28] needs more investigations.

In this work, a systematic DFT+U calculation for determining the magnetic ground state of PuO_2 is performed. The SOC effect is included explicitly in our calculations, which has been proved to be an essential effect in PuO_2.[35,36] Therefore, the noncollinear magnetic algorithm is employed here. Hubbard U model is used to describe the Coulomb interactions between correlated electrons. The whole process of this work can also be adopted to study other actinide oxides, such as UO_2, NpO_2, AmO_2, *etc*. The local density approximation (LDA),[37] the generalized gradient approximation (PBE here),[38] and the strongly constrained and appropriately normed (SCAN)[39] exchange–correlation functionals are applied in our calculations, respectively. The three exchange–correlation functionals which contain different physical information are belonging to three different levels of the Jacob ladder.[40] A pure *ab initio* DFT+U calculation without taking into account any experimental parameters is performed here.

2. Computational method

We employ the Vienna *ab initio* simulation package (VASP)[41] code to achieve DFT+U scheme. The projected augmented wave (PAW) method[42–44] with the frozen-core approximation is used. The first Brillouin zone of the unit cell is sampled by 6×6×6 k-point mesh. The cut-off energy of the plane wave basis for electron wave function is chosen as 520 eV. We have carefully checked the convergence of k-point mesh and cut-off energy. Atomic structures are fully relaxed until the Feynman–Hellman force on each atom is less than 0.01 eV/Å. The convergence accuracy of the energy for self-consistent calculation is 10^{-7} eV.

In the DFT+U study, screened Coulomb parameter U and Hund exchange parameter J are significant. Many efforts have been devoted to determine the U and J in PuO_2. By scanning lattice constant,[24,26,27] bulk modulus,[24,26] band gap,[20,27] and magnetic moment[20] in various U and J, the best combination of the two parameters can be chosen to match properties observed in experiments. Here, we adopt a scheme from a first-principles calculation[45] which points out the significance of electronic correlation on O-p orbits in actinide oxides. We note that a nonzero U for O-p does not change the properties of PuO_2 qualitatively. The electronic correlation on O-p orbits only slightly modifies the electronic structure (see supporting information S5). Thereby, $U = 4.7$ eV and $J = 0.6$ eV for Pu-5f orbits and $U = 3.0$ eV and $J = 0$ eV for O-p orbits are applied. Multiple values of U for Pu-f electrons have been used in the literature varying from 4 eV to 6.5 eV.[18,20,27,34–36] As a precaution, a test before further discussions is made and we find that the energy order of the magnetic structures keeps unchanged when U varies in the range of 3 eV to 7 eV. An unreasonable metallic ground state which is contrast to the experimental insulating state occurs only when U is quite small (roughly less than 0.5 eV).

We make use of the approach originated from Liechtenstein's[46] DFT+U method for the main part of the calculation. The generalized form of the energy functional is given by

$$\begin{aligned} &E_{\mathrm{DFT+U}}\left[\rho^{\sigma}(r),\{n^{\sigma}\}\right] \\ &= E_{\mathrm{DFT}}\left[\rho^{\sigma}(r)\right] + E^{U}\left[\{n^{\sigma}\}\right] - E_{\mathrm{dc}}\left[\{n^{\sigma}\}\right], \end{aligned} \tag{1}$$

where $\rho^{\sigma}(r)$ is the charge density, and n^{σ} is the trace of density matrix for spin σ ($\uparrow$ or $\downarrow$). The first term on the right-hand side represents standard DFT functional. It can be substituted by LDA, PBE, and SCAN functionals in our work. U and J affect the total energy independently in the double counting term written as

$$\begin{aligned} E_{\mathrm{dc}}\left[\{n^{\sigma}\}\right] = &\frac{1}{2}Un(n-1) \\ &-\frac{1}{2}J\left[n^{\uparrow}\left(n^{\uparrow}-1\right)+n^{\downarrow}\left(n^{\downarrow}-1\right)\right], \end{aligned} \tag{2}$$

where $n = n^{\uparrow} + n^{\downarrow}$ denotes the total occupation number of both spin-up and spin-down electrons. In addition, Dudarev's simplified DFT+U approach is also employed as a comparison, which will be discussed in Subsection 3.4.

3. Results

3.1. Magnetic structures in the cubic fluorite atomic structure

The Bravais lattice of PuO_2 is face centered cubic (FCC) with one Pu atom and two O atoms in the primitive cell. In order to produce possible 3*k* magnetic structures, the conventional cell (Pu_4O_8) of PuO_2 with the simple cubic (SC) lattice is adopted, as shown in the right top of Fig. 1. The four first-nearest Pu ions in this unit cell form a regular tetrahedron before relaxing the atomic structure with an imposed magnetic structure. Because of the periodic boundary condition, all second-nearest Pu ions are naturally in FM order. We cautiously do a test and prove that the unit cell adopted here is convincing to describe the magnetic ground state of PuO_2 (see more details in supporting information S1). The magnetic moments of O ions are ignored.

Based on former ideas,[2,20] typical magnetic structures are listed in Fig. 1. The superiority of our work is that three more collinear magnetic structures as shown in Figs. 1(e), 1(f), and 1(j) are involved in the calculations. The three magnetic structures are the transformations of transverse 1*k* AFM or longitudinal 1*k* AFM structures and they are discussed for the first time. With the existence of strong SOC and remarkable CF effect,[2] the magnetic anisotropy is very likely to play an important role in the formation of the magnetic ground state. As a result, we classify the magnetic structures into 001, 011, and 111 structures whose magnetic moments point along ⟨001⟩, ⟨011⟩, and ⟨111⟩, respectively. Details are shown in supporting information S2.

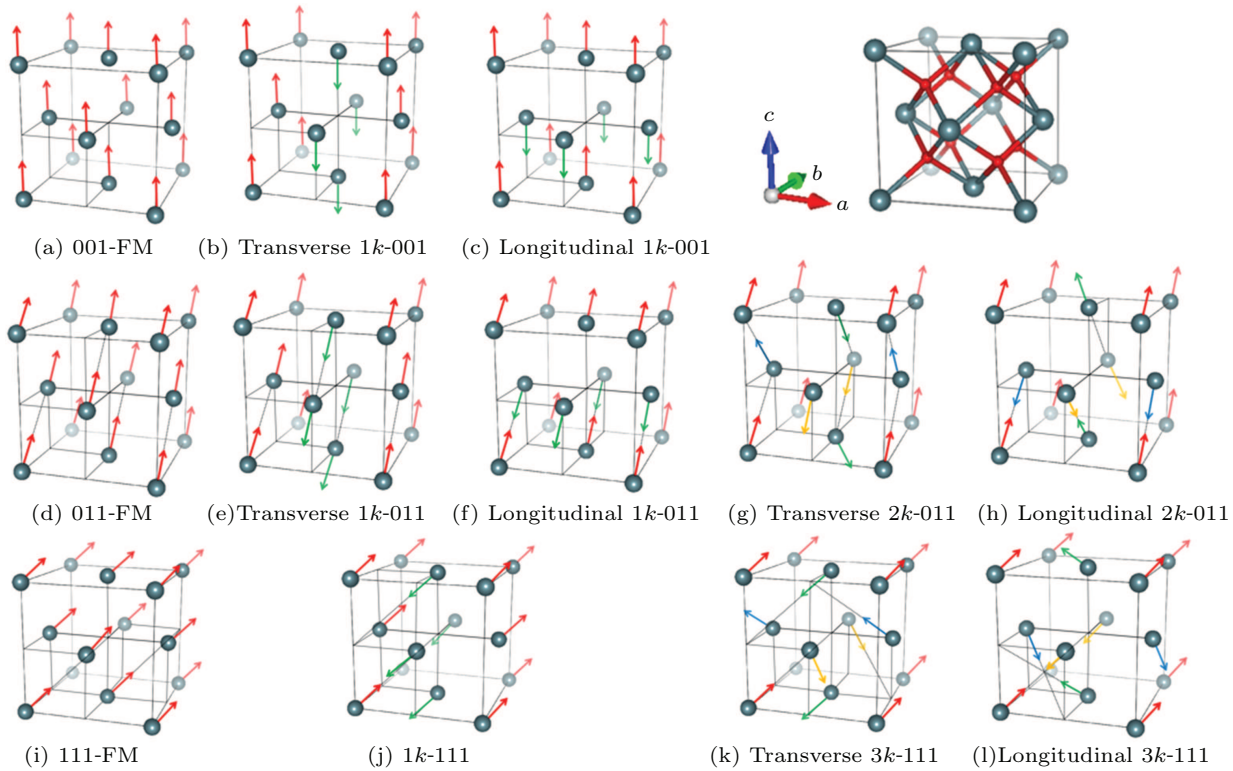


Fig. 1. The atomic structure of cubic fluorite PuO_2 (on the right top) and typical collinear and noncollinear magnetic structures [(a)–(l)]. Pu atoms represented by the large balls are shown to form magnetic structures. Arrows on the atoms represent magnetic moment vectors. Each color of the arrows corresponds to one specific vector of each magnetic structure. Orientations of the magnetic moments are along (a)–(c) ⟨001⟩, (d)–(h) ⟨011⟩, and (i)–(l) ⟨111⟩. The magnetic structures shown in panels (a), (d), and (i) are FM structures while the others are the so-called AFM structures with the label "AFM" omitted for simplicity.

3.2. Determination of the magnetic ground state

The atomic structure of actinide oxides tends to produce Jahn–Teller (JT) distortion when imposing a magnetic structure. For instance, the realistic UO_2 single crystal lowers the symmetry to $Pa\bar{3}$ space group at low temperature beneath the Néel temperature. The distortion on O atoms of about 0.014 Å along ⟨111⟩ has been observed within a transverse 3*k* magnetic structure.[3] This feature can also be faithfully reflected by our calculations performed on PuO_2. The space groups of the distorted crystal with different imposed magnetic structures are listed in Table 1. One can find that the nonmagnetic state and the longitudinal 3*k* magnetic state remain $Fm\bar{3}m$ space group recommended by the experiments. The transverse 3*k* magnetic state of PuO_2 is of $Pa\bar{3}$ symmetry. The distortion of O atoms is carefully calculated by employing the three functionals to be around 0.015 Å along ⟨111⟩. This phenomenon is very similar to that in UO_2. Meanwhile, imposing this distortion is far not enough to change the intrinsic magnetic ground state of PuO_2. Details can be found in supporting information S3. It indicates that the possible atomic distortion in actinide ox-

ides at low temperature is rather a consequence than an motive force of the magnetic structure for the ground state. Dudarev *et al*. have studied the JT distortion of UO_2 through LSDA+U calculations before.[47] Their conclusions and ours agree well with each other.

Lattice constant of PuO_2 calculated by LDA, PBE, SCAN, and HSE06[20] are compared in Fig. 2(a). One can see that different imposed magnetic structures only slightly modify the lattice constant. The notable distinction is contributed from the exchange–correlation functional. On one hand, LDA underestimates the lattice constant, while PBE (GGA) overestimates the lattice constant. This is consistent with prior LDA+U and GGA+U results.[26] On the other hand, HSE06 and especially SCAN give out pretty good prediction of the lattice constant.

The total magnetic moment of a Pu ion is composed of both spin moment and orbital moment originated from 5f electrons. Large magnetic dipole moment of the Pu ion is recommended as shown in Fig. 2(b). The magnetic moments of the Pu ions for different magnetic structures are approximately invariant in an acceptable range. This can be thought as a consequence of both strong SOC and on-site Coulomb interaction. These two effects dominate the local electronic configuration of the magnetic ions and tend to keep the magnetic moment unchanged. When rotating the local moments, only the electron–electron interactions between different sites are notably affected. This kind of interactions is relatively weak. As a result, different magnetic structures hardly make huge difference on the local magnetic moments of the Pu ions.

Table 1. Space group of PuO_2 with the magnetic structures imposed. These symmetry properties are only based on the simulated atomic structures. Any atomic distortion less than 10^{-3} Å is neglected. LDA, PBE, and SCAN as well as HSE06[20] give the consistent results here.

Magnetic structure	Space group	Magnetic structure	Space group
NM	$Fm\bar{3}m$ (225)	longitudinal 1k-011	$C2/m$ (12)
001-FM	$I4/mmm$ (139)	1k-111	$C2/m$ (12)
011-FM	$Immm$ (71)	transverse 2k-011	$Pbca$ (61)
111-FM	$R\bar{3}m$ (166)	longitudinal 2k-011	$I4/mmm$ (139)
Transverse 1k-001	$Fmmm$ (69)	transverse 3k-111	$Pa\bar{3}$(205)
Longitudinal 1k-001	$I4/mmm$ (139)	longitudinal 3k-111	$Fm\bar{3}m$ (225)
Transverse 1k-011	$Immm$ (71)		

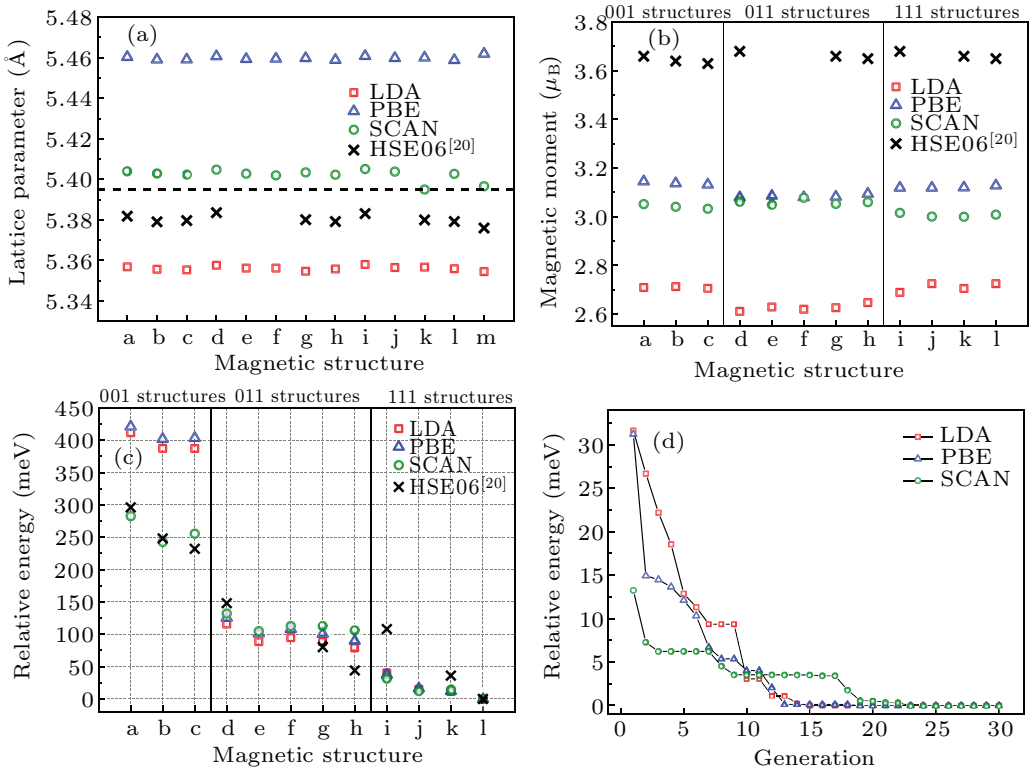


Fig. 2. (a) Lattice constant of PuO_2 with different magnetic structures calculated by LDA (red squares), PBE (blue triangles), SCAN (green circles), and HSE06 (black crosses).[20] In the abscissa, letters a–l correspond to magnetic structures shown in Figs. 1(a)–1(l), and m represents the nonmagnetic situation. Black dashed line denoting the experimental lattice constant from x-ray diffraction.[54] (b) The calculated magnetic moment of a single Pu ion with different magnetic structures imposed. Magnetic structures belonging to 001, 011, and 111 types are separated in three regions. (c) Relative energy of PuO_2 with different magnetic structures. Nonmagnetic state is not shown as it matches too much higher energy. The total energy of the magnetic ground state for each exchange–correlation functional is set to 0. (d) The lowest energy found in each generation relative to the energy of the magnetic ground state during the MagGene process.

The total energy of the Pu_4O_8 unit cell varies in a range of about 420 meV among the magnetic structures as shown in Fig. 2(c). The energy of the nonmagnetic state in our calculations is almost about 4 eV higher than the other magnetic states no matter which exchange–correlation functional is applied (LDA, PBE, SCAN, as well as HSE06[20]). Thereby, we do not discuss the simulated nonmagnetic states in this work. According to the results for LDA, PBE, and SCAN, the orientation of the local magnetic moments dominate the total energy as we expected. The 111 structures are normally favored in energy and the 011 structures take higher energy than the 111 structures. Finally, the 001 structures cause much higher energy than both 111 structures and 011 structures. Furthermore, the FM configuration (*i.e.*, structures a, d, and i) is also less stable than AFM configuration in a group of structures whose magnetic moments point along the same crystallographic direction family (for $\langle 001\rangle$, $\langle 011\rangle$, and $\langle 111\rangle$, respectively). In the case of HSE06,[20] things are a little different. Referring to Fig. 2(c), relative energy of the magnetic structures shows a similar trend to our applied three functionals. However, we notice that the departure in energy between FM structures and AFM structures is larger. From this point of view, HSE06 hybrid functional may take more highly of the interactions from f–p super-exchange and f–f exchange than the other three functionals. Anyway, the longitudinal 3*k* AFM structure to be the magnetic ground state of PuO_2 is confirmed by LDA, PBE, SCAN, and HSE06 consistently.

When SOC is involved in DFT + *U* calculations, total energy is not only the functional of the charge density but also the functional of the magnetization density when no external field is imposed.[48] The magnetic moment of an ion on site *i* is the integral of the magnetization density inside the Wigner–Seitz (WS) radius given by

$$\boldsymbol{M}_i = \int_{\mathrm{WS}} \boldsymbol{M}(\boldsymbol{r})\,\mathrm{d}r^3. \tag{3}$$

In our unconstrained DFT + *U* + SOC calculations realized by VASP,[41] the orientation of the initial local magnetic moment is still needed to be artificially set. Usually, to search the ground state in the subspace of magnetic ordered states, several typical high-symmetry magnetic structures are at least needed to be considered (refer to Fig. 1). In this way, the number of considered magnetic structures is limited. To exclude any other possible magnetic structures with lower energy which might be missed, we expand the searching range to a larger space. We firstly let the local moments in the unit cell rotate freely. Random magnetic structures can be then gained at different moments. Meanwhile, to overcome the blindness during the calculations, the MagGene code based on the genetic algorithm is applied to locate the magnetic ground state efficiently. Details can be found in supporting information S4 and also the paper from Zheng *et al.*[49] At the beginning of the searching process for PuO_2, sixteen random magnetic structures are generated. Following that, five structures with the lowest five energies are chosen as parents for the next generation. Based on these parents, six mutation structures and two crossover structures are produced. The last part of the next generation is eight $(16-6-2=8)$ random structures, which help to get rid of the local minima of the energy surface and keep the size of population unchanged. The lowest energy found in each generation is shown in Fig. 2(d). When a thirty generations' searching is finished, the longitudinal 3*k* AFM ground state is found in the 19th, 22nd, and 23rd generations when LDA, PBE, and SCAN are applied, respectively.

3.3. Electronic structure of the magnetic ground state

A large unit cell of PuO_2 is necessary to describe the longitudinal 3*k* AFM ground state. The first Brillouin zone of the Pu_4O_8 simple cubic lattice is shown in Fig. 3.

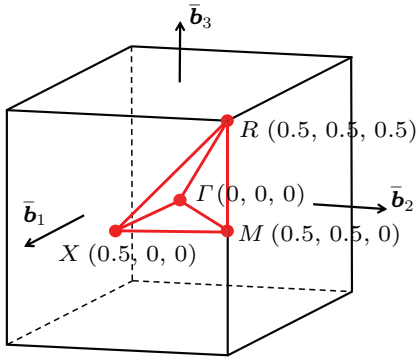


Fig. 3. First Brillouin zone and high symmetry path for the simple cubic lattice of the Pu_4O_8 conventional cell.

We adopt Γ–*X*–*M*–Γ–*R*–*X*/*M*–*R* high symmetry path[50] to describe the dispersion of the total energy. Density of states (DOS) and electronic band structures calculated by the three functionals are plotted in Fig. 4. Our DFT + *U* + SOC calculations for the longitudinal 3*k* AFM ground state reasonably suggest PuO_2 to be a charge-transfer insulator which has been widely identified before. A strong hybridization between Pu-f and O-p orbits is identified. This feature explains why taking into account the correlation on O-p orbits is necessary. Similar to the magnetic ground state calculated by HSE06,[20] a remarkable peak of O-p below the Fermi level in the DOS is located at about −1.1 eV. Another broad peak close to the Fermi level is actually a double peak in our calculation as shown in Figs. 4(a)–4(c). One can see from the Figs. 4(d)–4(f) that the direct gap of the band structure is 2.46 eV, 2.47 eV, and 2.69 eV corresponding to the LDA, PBE, and SCAN functionals. To our surprise, these values calculated from the longitudinal 3*k* AFM ground state are even more close to the experimental optical gap which is 2.8 eV[51] than that from the simulated nonmagnetic state (about 1.8 eV).[18,36] Hence, we trust that the longitudinal 3*k* AFM structure is the best approximation to model the electronic ground state of PuO_2 so far and it has been adopted to calculate the formation energy.[47]

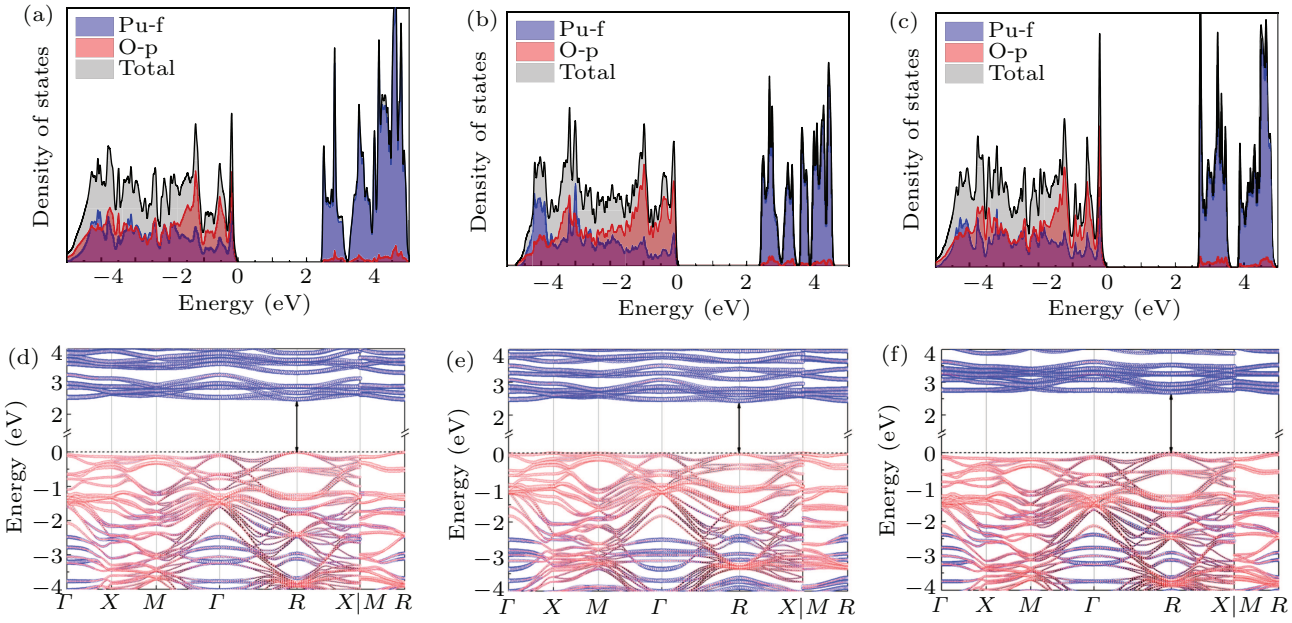


Fig. 4. Electronic DOS of the longitudinal 3*k* AFM ground state and the corresponding band structures for LDA [(a) and (d)], PBE [(b) and (e)], and SCAN [(c) and (f)]. Blue circles and red circles in panels (d)–(f) represent the contributions from Pu-f and O-p orbitals. The size of the circles shows the weight of each component.

3.4. A comparison with Dudarev's DFT + *U* approach

Another widely used DFT + *U* scheme based on Dudarev's DFT + *U* model[52] is inspected here. The total energy modified by this model is given by

$$E_{\mathrm{DFT}+U} = E_{\mathrm{DFT}} + \frac{(U-J)}{2}\sum_{\sigma}\left[\mathrm{Tr}\rho^{\sigma} - \mathrm{Tr}\left(\rho^{\sigma}\rho^{\sigma}\right)\right], \quad (4)$$

where ρ^{σ} is the density matrix of correlated electrons with spin σ. In this simplified approach, U and J are handled in a spherically averaged form of the screened Coulomb interaction and exchange interaction. We adopt the same U and J as used in the former Liechtenstein's model. Total energies of different magnetic structures are calculated again, and the corresponding results are shown in Fig. 5(a). We firstly find that the energy range among these structures is about 200 meV, which is only about half of that obtained by Liechtenstein's approach. For LDA or PBE functional, the ⟨111⟩ easy axis of magnetization is reproduced and the longitudinal 3*k* magnetic ground state is determined as expected. However, for SCAN functional, structures with atomic moments along ⟨011⟩ are favored in energy.

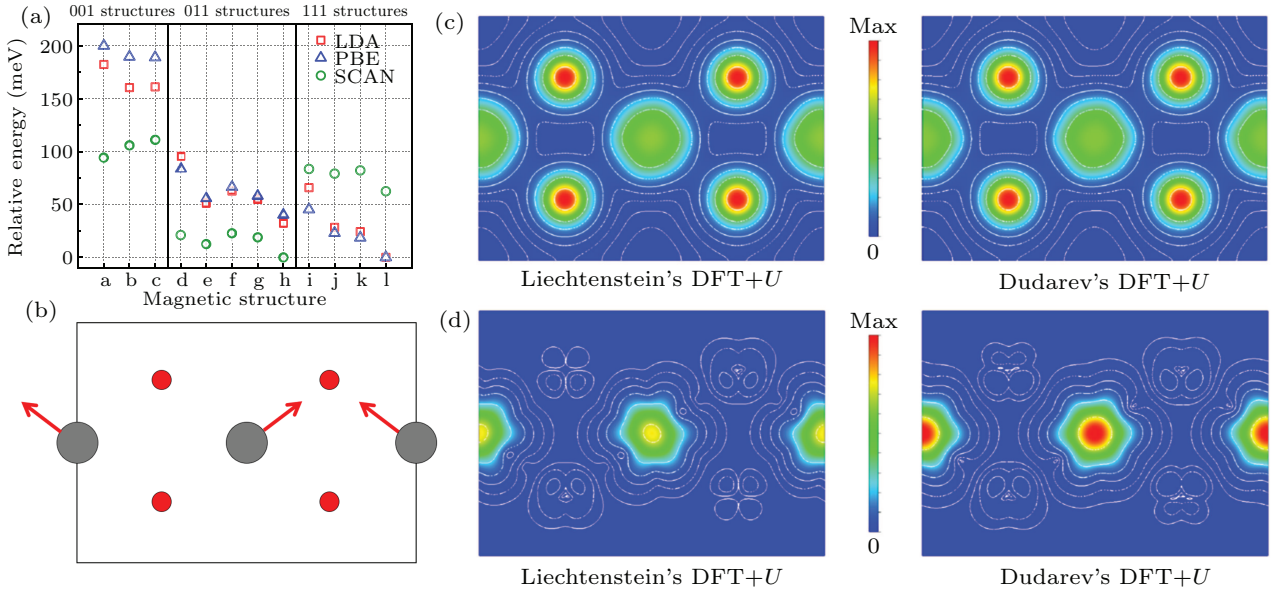


Fig. 5. (a) Relative energy of PuO_2 with different magnetic structures obtained from Dudarev's DFT + *U* approach. In the abscissa, letters a–l correspond to the magnetic structures shown in Figs. 1(a)–1(l). The total energy of the magnetic ground state for each exchange–correlation functional is set to 0. (b) The (1 −1 0) section of PuO_2 crystal with longitudinal 3*k* AFM structure. Red arrows represent magnetic moments. (c) The charge density plot on the (1 −1 0) section calculated by Liechtenstein's DFT + *U* approach and Dudarev's DFT + *U* approach. (d) The magnetization densities plot on the (1 −1 0) section calculated by Liechtenstein's DFT + *U* approach and Dudarev's DFT + *U* approach. The direction of the magnetization vector on each grid is not shown for simplicity.

Moreover, the preference for AFM structures in energy is invalid in this case. As shown in Fig. 5(a), the 001-FM structure is the most stable among 001 magnetic structures. In Dudarev's DFT+U approach, it is abnormal for SCAN to get such results which are contrary to LDA and PBE, especially when a consistent conclusion is arrived with Liechtenstein's DFT+U approach for all three exchange–correlation functionals.

We also would like to compare the ionic states of the longitudinal 3k magnetic structure calculated by Liechtenstein's DFT+U approach and Dudarev's DFT+U approach. The charge densities of both approaches with SCAN adopted are represented in Fig. 5(c). There is only slight difference in the two charge densities, which is originated from Pu ions. However, the magnetization density emphasizes a remarkable distinction. By calculating the integral of the magnetization density inside the Wigner–Seitz radius of Pu, we obtain the magnetic moment to be 3.00 μ_B and 3.72 μ_B from Liechtenstein's approach and Dudarev's approach. From the distributions of the magnetization densities as shown in Fig. 5(d), we notice that two different ionic states are gained from these two DFT+U approaches although the same values of U and J are employed. The corresponding occupation matrices for Pu-f orbits are also shown in supporting information S6 to numerically confirm this character.

4. Discussion

We treat PuO_2 as a standard computational model of actinide oxides with half-filled 5f electrons and expect the methodology here to be expanded to other actinide oxides. Previous DFT calculations have illustrated that a simple collinear magnetic model without SOC is meaningful to describe a series of properties of PuO_2 as long as a Hubbard U modification is considered. However, this framework of computation is too rough for magnetic properties. With the existence of the on-site Coulomb U and strong SOC, the way of occupation for Pu-5f orbits takes on great responsibilities for the total energy. On our calculated NM state, the electronic configuration of the 5f electrons remarkably differs from the magnetic states and that's why it has much higher energy. Based on the same local occupation for Pu-5f orbits, the total charge density and the magnetization density can be once again modified by a specific magnetic structure. According to our simulations, the total energies slightly fluctuate among different magnetic structures in a range of dozens of meV per PuO_2.

We point out that the typical magnetic structures here combined with their energies can be used to fit an effective pseudo spin Hamiltonian as proposed before.[53] Since the spin-spin interactions in actinide oxides are complex, multiple model parameters have been taken into account in the Hamiltonian. As a result, for the accuracy of the fitting job, the amount of the used magnetic structures should not be too small. Meanwhile, the magnetic structures ought to be with the approximately equal local electronic occupation for Pu-5f orbits. Once any magnetic structures with definitely different ionic states are involved in the fitting job, the fitted parameters would be unphysical and meaningless. At least for PuO_2, the magnetic structures simulated by our DFT+U method are perfect samples for a high-quality fitting.

Furthermore, there are at least two possible reasons need to be noticed for understanding the inconsistency of the ground states between DFT calculation and experiments for PuO_2. The first reason is that the longitudinal 3k magnetic state obtained here may be a metastable state which corresponds to a local minima on the energy surface. To validate this, an occupation control procedure for the local electrons should be a promising method to completely search the subspace of the electronic configuration. Another reason is that the physical information of the computational model may be not compatible with the real system. If so, additional modification is required for DFT based calculations to PuO_2. Anyway, the origin of this inconsistency needs more intriguing investigations. An universal *ab initio* computational framework is needed to reasonably describe the real ground state of actinide oxides based on DFT+U method. We will leave this issue to our long-term work.

5. Conclusions

We studied the magnetic ordered states of PuO_2 by using DFT+U method with SOC included. The LDA, PBE, and SCAN exchange–correlation functionals are applied, respectively. The typical magnetic structures in the cubic fluorite crystal structure are classified and labeled. The JT distortions are simulated, which can be seen as an appendage of the imposed magnetic structure. The orientations of the local moments in the crystal environment are found to play an important role in the contribution to the total energy. Beyond the usual searching procedure of the magnetic ground state, the MagGene code based on the genetic algorithm is employed to ensure the longitudinal 3k AFM ground state recommended by all the three functionals. After that, the electronic structure of the magnetic ground state is discussed. According to our calculations, PuO_2 is predicted to be a charge-transfer insulator, whose optical gap agrees well with the experimental value. We believe that the longitudinal 3k AFM structure should be a good approximation to model the magnetic ground state of PuO_2. All these results obtained here are in reasonable agreement with that obtained by using a hybrid functional in the prior computational work. Finally, we notice a divergence between Liechtenstein's DFT+U approach and Dudarev's DFT+U approach when both are applied to

PuO_2. This phenomenon occurs only when SCAN exchange–correlation functional is adopted.

Acknowledgements

Project supported by National Natural Science Foundation of China, (Grant No. 12104034).

We thank professor Fa-Wei Zheng from the School of Physics of Beijing Institute of Technology for his advice to this work. We also thank professor James T. Pegg from Department of Chemistry of University College London for his useful discussion with us.

References

[1] Haschke J M, Allen T H and Morales L A 2000 *Science* **287** 285
[2] Santini P, Lémanski R and Erdös P 1999 *Adv. Phys.* **48** 537
[3] Faber J and Lander G H 1976 *Phys. Rev. B* **14** 1151
[4] Desgranges L, Ma Y, Garcia P, Baldinozzi G, Simeone D and Fischer H E 2017 *Inorg. Chem.* **56** 321
[5] Blackburn E, Caciuffo R, Magnani N, Santini P, Brown P J, Enderle M and Lander G H 2005 *Phys. Rev. B* **72** 184411
[6] Wilkins S B, Paixão J A, Caciuffo R, Javorsky P, Wastin F, Rebizant J, Detlefs C, Bernhoeft N, Santini P and Lander G H 2004 *Phys. Rev. B* **70** 214402
[7] Tokunaga Y, Homma Y, Kambe S, Aoki D, Sakai H, Yamamoto E, Nakamura A, Shiokawa Y, Walstedt R E and Yasuoka H 2005 *Phys. Rev. Lett.* **94** 137209
[8] Santini P, Carretta S, Magnani N, Amoretti G and Caciuffo R 2006 *Phys. Rev. Lett.* **97** 207203
[9] Tokunaga Y, Aoki D, Homma Y, Kambe S, Sakai H, Ikeda S, Fujimoto T, Walstedt R E, Yasuoka H, Yamamoto E, Nakamura A and Shiokawa Y 2006 *Phys. Rev. Lett.* **97** 257601
[10] Arrott A and Goldman J E 1957 *Phys. Rev.* **108** 948
[11] Ross J W and Lam D J 1967 *J. Appl. Phys.* **38** 1451
[12] Raphael G and Lallement R 1968 *Solid State Commun.* **6** 383
[13] Yasuoka H, Koutroulakis G, Chudo H, Richmond S, Veirs D K, Smith A I, Bauer E D, Thompson J D, Jarvinen G D and Clark D L 2012 *Science* **33** 6083
[14] Tokunaga Y, Sakai H, Fujimoto T, Kambe S, Walstedt R E, Ikushima K, Yasuoka H, Aoki D, Homma Y, Haga Y, Matsuda T D, Ikeda S, Yamamoto E, Nakamura A, Shiokawa Y, Nakajima K, Arai Y and Onuki Y 2007 *J. Alloys Compd.* **444–445** 241
[15] Martel L, Magnani N, Vigier J F, Boshoven J, Selfslag C, Farnan I, Griveau J C, Somers J and Fanghanel T 2014 *Inorg. Chem.* **53** 6928
[16] Kern S, Robinson R A, Nakotte H, Lander G H, Cort B, Watson P and Vigil F A 1999 *Phys. Rev. B* **59** 104
[17] Colarieti-Tosti M, Eriksson O, Nordström L, Wills J and Brooks M S S 2002 *Phys. Rev. B* **65** 195102
[18] Shick A B, Koloren J, Havela L, Gouder T and Caciuffo R 2014 *Phys. Rev. B* **89** 041109
[19] Gendron F and Autschbach J 2017 *J. Phys. Chem. Lett.* **8** 673
[20] Pegg J T, Shields A E, Storr M T, Wills A S, Scanlon D O and de Leeuw N H 2019 *Phys. Chem. Chem. Phys.* **20** 20943
[21] Noe M and Fuger J 1974 *Inorg. Nucl. Chem. Lett.* **10** 7
[22] Ansoborlo E, Prat O, Moisy P, Auwer C D, Guilbaud P, Carriere M, Gouget B, Duffield J, Doizi D, Vercouter T, Moulin C and Moulin V 2006 *Biochimie* **88** 1605
[23] Tokunaga Y, Sakai H, Fujimoto T, Kambe S, Walstedt R E, Ikushima K, Yasuoka H, Aoki D, Homma Y, Haga Y, Matsuda T D, Ikeda S, Yamamoto E, Nakamura A, Shiokawa Y, Nakajima K, Arai Y and Ōnuki Y 2007 *J. Alloys Compd.* **444–445** 241
[24] Zhang P, Wang B T and Zhao X G 2010 *Phys. Rev. B* **82** 144110
[25] Prodan I D and Scuseria G E 2005 *J. Chem. Phys.* **123** 014703
[26] Sun B, Zhang P and Zhao X G 2008 *J. Chem. Phys.* **128** 084705
[27] Jomard G, Amadon B, Bottin F and Torrent M 2008 *Phys. Fev. B* **78** 075125
[28] Jollet F, Jomard G and Amadon B 2009 *Phys. Rev. B* **80** 235109
[29] Shi H L, Chu M F and Zhang P 2010 *J. Nucl. Mater.* **400** 151
[30] Wang B T, Zheng J J, Qu X, Li W D and Zhang P 2015 *J. Alloys Compd.* **628** 267
[31] Minamoto S, Kato M, Konashi K and Kawazoe Y 2009 *J. Nucl. Mater.* **385** 18
[32] Sun B, Liu H F, Song H F, Zhang G C, Zheng H, Zhao X G and Zhang P 2012 *J. Nucl. Mater.* **426** 139
[33] Moten S A, Atta-Fynn R, Ray A K and Huda M N 2016 *J. Nucl. Mater.* **468** 37
[34] Jomard G and Bottin F 2011 *Phys. Rev. B* **84** 195469
[35] Nakamura H, Machida M and Kato M 2010 *Phys. Rev. B* **82** 155131
[36] Suzuki M T, Magnani N and Oppeneer P M 2013 *Phys. Rev. B* **88** 195146
[37] Kohn W and Sham L J 1965 *Phys. Rev.* **140** A1133
[38] Perdew J P, Burke K and Wang Y 1996 *Phys. Rev. B* **54** 16533
[39] Sun J W, Ruzsinszky A and Perdew J P 2015 *Phys. Rev. Lett.* **115** 036402
[40] Perdew J P, Ruzsinszky A, Tao J, Staroverov V N, Scuseria G E and Csonka G I 2005 *J. Chem. Phys.* **123** 062201
[41] Kresse G and Furthmuller J 1996 *Phys. Rev. B* **54** 11169
[42] Blöchl P E 1994 *Phys. Rev. B* **50** 17953
[43] Kresse G and Joubert D 1999 *Phys. Rev. B* **59** 1758
[44] Blöchl P E, Först C J and Schimpl J B 2003 *Bull. Mater. Sci.* **26** 33
[45] Morée J B, Outerovitch R and Amadon B 2021 *Phys. Rev. B* **103** 045113
[46] Liechtenstein A I, Anisimov V V and Zaanen J 1995 *Phys. Rev. B* **52** R5467
[47] Neilson W D, Pegg J T, Steele H and Murphy S T 2021 *Phys. Chem. Chem. Phys.* **23** 4544
[48] Jansen H J F 1999 *Phys. Rev. B* **59** 4699
[49] Zheng F W and Zhang P 2021 *Compt. Phys. Commun.* **259** 107659
[50] Setyawan W, Curtarolo S 2010 *Comput. Mater. Sci.* **49** 299
[51] McCleskey T M, Bauer E, Jia Q, Burrell A K, Scott B L, Conradson S D, Mueller A, Roy L, Wen X D, Scuseria G E and Martin R L 2013 *J. Phys. Appl.* **113** 013515
[52] Dudarev S L, Botton G A, Savrasov S Y, Humphreys C J and Sutton A P 1998 *Phys. Rev. B* **57** 1505
[53] Dudarev S L, Liu P, Andersson D A, Stanek C R, Ozaki T and Franchini C 2019 *Phys. Rev. Mater.* **3** 083802
[54] Yamashita T, Nitani N, Tsuji T and Inagaki H 1997 *J. Nucl. Mater.* **245** 72